
JOURNAL OF THE AMERICAN CHEMICAL SOCIETY

Direct Observation of Aminoglycoside–RNA Interactions by Surface Plasmon Resonance

Martin Hendrix, E. Scott Priestley, Gerald F. Joyce and Chi-Huey Wong*

Contribution from the Department of Chemistry and The Skaggs Institute of Chemical Biology,
The Scripps Research Institute, 10550 North Torrey Pines Road, La Jolla, California 92037

Received December 13, 1996[⊗]

Abstract: The specificity of neomycin B and related aminoglycoside antibiotics in their interaction with the Rev responsive element (RRE) of HIV-1 mRNA has been studied by directly observing the aminoglycoside–RNA complexes using surface plasmon resonance. Several different RNA sequences, each with a biotin tag, have been prepared using T7 RNA polymerase-catalyzed transcription of synthetic DNA templates and have been immobilized on a streptavidin-coated surface for the binding study. The results indicate that neomycin B is not specific for the G-rich bubble region in RRE. Rather, it appears to interact with three different sites, each with a submicromolar dissociation constant, within the 67-nucleotide domain II of RRE. Further analysis of neomycin B binding with three short synthetic RNA hairpins showed binding with submicromolar affinity and 1:1 stoichiometry in each case. This suggests that neomycin B may generally bind with this affinity to regular A-form RNA or hairpin loops. The approach described here is generally useful for understanding the fundamental interactions involved in the specific recognition of nucleic acids by small molecules which is the basis of rational drug design.

Targeting specific RNA sequences with small-molecule drugs is a potentially attractive approach to the therapy of many diseases. Aminoglycosides (Figure 1) belong to the small group of low molecular weight compounds known to date that bind selectively to specific RNA sequences.¹ Neomycin B and related structures, for example, have been shown to bind two important regulatory domains in HIV-1 mRNA, the Rev responsive element (RRE),² and the *trans*-activation response element (TAR),³ and to inhibit binding of their cognate proteins

Rev and Tat, respectively. By facilitating the nuclear export and subsequent expression of unspliced or partially spliced mRNAs, Rev acts as a crucial switch between viral latency and active viral replication.^{4–6} We are interested in developing inhibitors of the interaction between RRE and its cognate protein Rev as potential therapeutics against HIV.⁷ However, despite the promising activity of some aminoglycosides, little is known

[⊗] Abstract published in *Advance ACS Abstracts*, April, 1, 1997.

(1) (a) Wilson, W. D.; Ratmeyer, L.; Zhao, M.; Strekowski, L.; Boykin, D. *Biochemistry* **1993**, *32*, 4098. (b) McConnaughie, A. W.; Spychala, J.; Zhao, M.; Boykin, D.; Wilson, W. D. *J. Med. Chem.* **1994**, *37*, 1063. (c) Zhao, M.; Ratmeyer, L.; Peloquin, R. G.; Yao, S.; Kumar, A.; Spychala, J.; Boykin, D. W.; Wilson, W. D. *Bioorg. Med. Chem.* **1995**, *3*, 785. (d) Fernandez-Saiz, M.; Schneider, H.-J.; Sartorius, J.; Wilson, W. D. *J. Am. Chem. Soc.* **1996**, *118*, 4739.

(2) (a) Zapp, M. L.; Stern, S.; Green, M. R. *Cell* **1993**, *74*, 969. (b) Werstuck, G.; Zapp, M. L.; Green, M. R. *Chem. Biol.* **1996**, *3*, 129.

(3) Mei, H.-Y.; Galan, A. A.; Halim, N. S.; Mack, D. P.; Moreland, D. W.; Sanders, K. B.; Truong, H. N.; Czarnik, A. W. *Bioorg. Med. Chem. Lett.* **1995**, *5*, 2755.

(4) (a) Zapp, M. L.; Green, M. R. *Nature* **1989**, *342*, 714–716. (b) Daly, T. J.; Cook, K. S.; Gray, G. S.; Maione, T. E.; Rusche, J. R. *Nature* **1989**, *342*, 816–819.

(5) (a) Malim, M. H.; Hauber, J.; Le, S.-Y.; Maizel, J. V.; Cullen, B. R. *Nature* **1989**, *338*, 254–257. (b) Malim, M. H.; Cullen, B. R. *Mol. Cell. Biol.* **1993**, *13*, 6180–6189. (c) Fischer, U.; Meyer, S.; Teufel, M.; Heckel, C.; Lührmann, R.; Rautmann, G. *EMBO J.* **1994**, *13*, 4105–4112.

(6) Wen, W.; Meinkoth, J. L.; Tsien, R. Y.; Taylor, S. S. *Cell* **1995**, *82*, 463. (b) Fischer, U.; Huber, J.; Boelens, W. C.; Mattaj, I. W.; Lührmann, R. *Cell* **1995**, *82*, 475. (c) Bogerd, H. P.; Fridell, R. A.; Madore, S.; Cullen, B. R. *Cell* **1995**, *82*, 485. (d) Stutz, F.; Neville, M.; Rosbach, M. *Cell* **1995**, *82*, 495.

(7) Park, W. K. C.; Auer, M.; Jaksche, H.; Wong, C.-H. *J. Am. Chem. Soc.* **1996**, *118*, 10150.

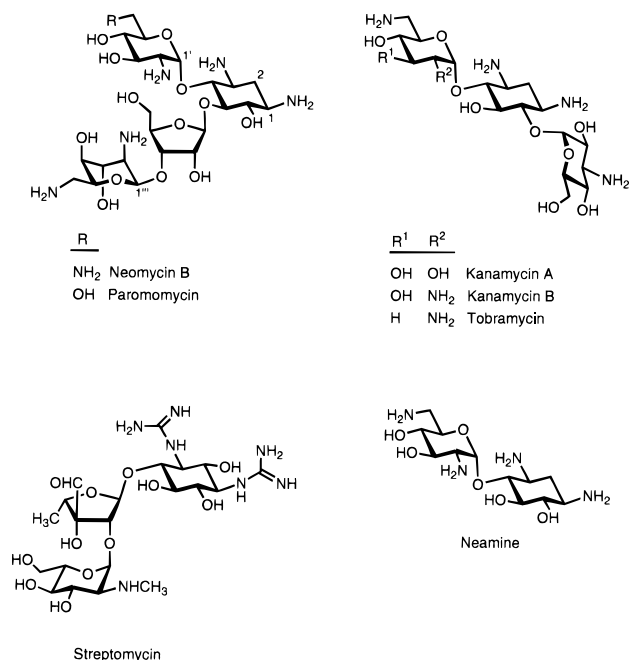


Figure 1. Structure of aminoglycosides. The neomycin family is characterized by a 2-deoxystreptamine–cyclitol core. Streptomycin belongs to a different family of aminoglycosides and is characterized by its guanidinium groups.

about the factors governing their affinity and specificity for particular RNA structures, thus hindering rational drug development.

A crucial element in understanding aminoglycoside–RNA recognition is the development of detailed structure–activity relationships and the analysis of sequence specificity. Frequently, protein binding to nucleic acids is evaluated by gel mobility shift⁸ or filter binding⁹ assays. For small molecules, however, complexes with RNA are often difficult to observe directly. Instead, they are usually screened in a competition assay in the presence of an RNA binding protein. *In this type of competition assay, however, it is impossible to test for specificity, i.e., the ability to discriminate between different RNA sequences.* Therefore, we have developed a novel assay based on surface plasmon resonance (SPR) that allows the direct observation of aminoglycoside–RNA interactions and is able to test for specificity.

SPR is an optical phenomenon that can be used to detect binding to ligands that are immobilized on special SPR sensorchip surfaces. The observed SPR signal correlates to mass concentration near the surface, allowing binding to immobilized ligands to be monitored. Depending on the experimental design, both thermodynamic and kinetic information can be derived. SPR has been applied to the direct monitoring of a wide range of macromolecular interactions,¹⁰ but only recently have technical improvements in the accuracy of detection put the analysis of small-molecule binding within reach. We have developed a general SPR-based method for monitoring small-molecule–RNA interactions. Specifically, we have synthesized several 5′-biotinylated RNA transcripts and immobilized them on the surface of streptavidin-coated sensorchips. Using this system, we were able to study in detail the binding of aminoglycoside antibiotics to these sequences (Figure 2). Analysis of the

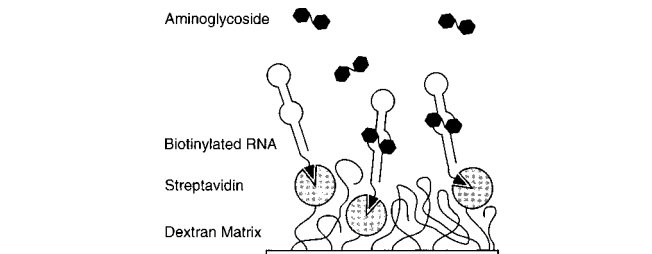
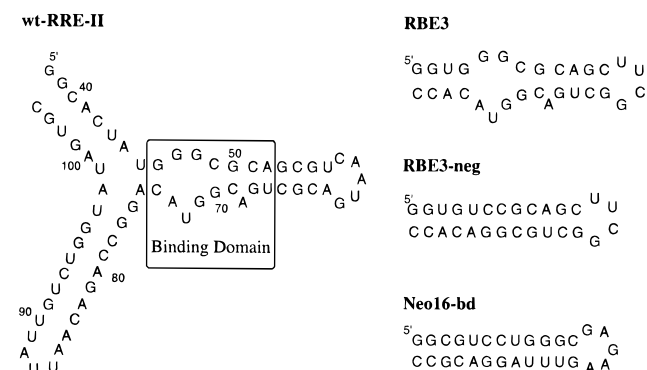


Figure 2. SPR sensorchip surface presenting immobilized RNA hairpins. Streptavidin is covalently attached to the carboxymethyl dextran matrix *via* amide linkages. RNA sequences are then non-covalently immobilized through their 5′-biotin termini.

binding data has allowed us to gain new insights into aminoglycoside–RNA interactions.

Results

We have examined three different sequences related to RRE. The first sequence is the wild type domain II of RRE (wt-RRE-II) which contains the high-affinity Rev-protein-binding site of RRE.¹¹ The second sequence is the abbreviated 30-nucleotide stem-loop RBE3,¹² which still contains the essential elements for Rev recognition¹³ and which has been shown to bind Rev-derived peptides with high specificity. Its structure, both in solution and in the peptide-complexed form, has been determined by NMR.¹⁴ The G-rich bubble which is partially closed by the formation of purine–purine base pairs widens the major groove enough to accommodate the α -helical RNA-binding domain of Rev. On the basis of footprinting experiments, it has been suggested that the G-rich bubble in this sequence is also the binding site for neomycin B.^{2a} The third RRE-related sequence is a designed hairpin, RBE3-neg, where the Rev-binding site has been disrupted by mutating the bubble region. This was accomplished by deleting two looped out nucleotides, A68 and U72 (wt-numbering), and changing the two purine–purine base pairs, G47:A73 and G48:G71, to standard Watson–Crick pairs. Finally, we have included Neo16bd, a neomycin B binding sequence that is not related to RRE and consequently is not expected to bind Rev. This sequence is derived from an RNA–aptamer that was selected to bind neomycin B.¹⁵



Synthesis and Immobilization of RNAs. Biotin–RNA conjugates were prepared as shown in Scheme 1. *In vitro*

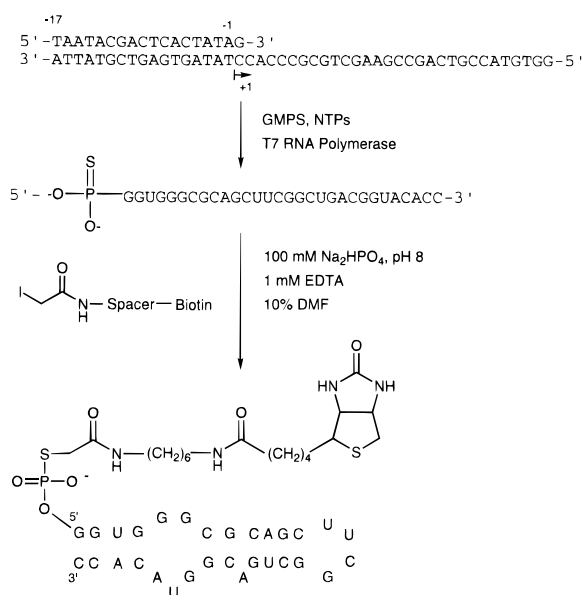
(8) Revzin, A. *BioTechniques* **1989**, *7*, 346.

(9) (a) Clore, G. M.; Gronenborn, A. M.; Davies, R. W. *J. Mol. Biol.* **1982**, *155*, 447. (b) Woodbury, C. P., Jr.; von Hippel, P. H. *J. Am. Chem. Soc.* **1983**, *22*, 4730.

(10) Malmquist, M. *Nature* **1993**, *361*, 186.

(11) (a) Heaphy, S.; Dingwall, C.; Ernberg, I.; Gait, M. J.; Green, S. M.; Karn, J.; Lowe, A. D.; Singh, M.; Skinner, M. A. *Cell* **1990**, *60*, 685–693. (b) Malim, M. H.; Tiley, L. S.; McCarn, D. F.; Rusche, J. R.; Hauber, J.; Cullen, B. R. *Cell* **1990**, *60*, 675–683. (c) Olsen, H. S.; Nelbock, P.; Cochrane, A. W.; Rosen, C. A. *Science* **1990**, *247*, 845–848. (d) Holland, S. M.; Ahmad, N.; Maitra, R. K.; Wingfield, P.; Venkatesan, S. *J. Virol.* **1990**, *64*, 5966–5975. (e) Heaphy, S.; Finch, J. T.; Gait, M. J.; Karn, J.; Singh, M. *Proc. Natl. Acad. Sci. U.S.A.* **1991**, *88*, 7366–7370. (f) Kjemis, J.; Brown, M.; Chang, D. D.; Sharp, P. A. *Proc. Natl. Acad. Sci. U.S.A.* **1991**, *88*, 683–687.

Scheme 1. Synthesis of RNA-5'-Phosphorothioates by *In Vitro* Transcription with T7 RNA Polymerase in the Presence of GMPS, Followed by Biotinylation with a Biotin–Iodoacetamide Derivative That Allows Specific Immobilization



transcription of a DNA template in the presence of guanosine-5'-monophosphorothioate (GMPS), catalyzed by T7 RNA polymerase,¹⁶ produced a 5'-phosphorothioate–RNA oligonucleotide. Subsequent modification with an extended biotin–iodoacetamide reagent gave the desired 5'-biotinylated RNA. As shown in Figure 3A for the case of RBE3, 5'-phosphorothioate oligonucleotides are quantitatively modified with biotin, while 5'-phosphates are unreactive, demonstrating selective reaction at the single sulfur atom. This approach should be generally useful for the preparation of a wide range of specifically modified RNA sequences.

When streptavidin-coated sensorchips were exposed to solutions of gel-purified, biotinylated RNA oligomers, time-dependent stable immobilization was observed (Figure 3B). Rigorous purification of the 5'-biotinylated RNAs by gel electrophoresis to remove excess biotinylation reagent was critical for successful immobilization. Simple ethanol precipitation was not sufficient for this purpose and resulted in low levels of captured RNA. During the optimization of the immobilization parameters to reduce consumption of the RNA conjugates, we found that lowering the pH from 7.4 to 6.8 resulted in substantially higher levels of immobilization. This is presumably due to improved preconcentration of the negatively charged biotin–RNA conjugates at the streptavidin-coated surface (pI 5–6). The immobilization was specific for biotinylated sequences, as unbiotinylated RBE3–5'-phosphorothioate did not lead to any

appreciable capture of RNA ligand (<5 RU, lower trace in Figure 3B). Immediately following exposure to the unbiotinylated RNA, biotinylated RBE3 was injected into the same flow cell, resulting in the usual level of functionalization (ca. 580 RU, upper trace in Figure 3B). Furthermore, immobilization is dependent on the level of streptavidin loading. In a gradient sensorchip having four different levels of streptavidin loading, the amount of captured biotin–RNA was proportional to the streptavidin loading levels (data not shown). Taken together, these observations clearly demonstrate that biotin–RNA conjugates are specifically immobilized on the surface through the streptavidin linker.

Binding of RNAs to Rev Peptide. To establish that the immobilized RNA was properly folded, we investigated the binding of the four RNA sequences to Rev27 (Figure 4). This synthetic peptide contains the α -helical RNA-binding domain of Rev protein (Rev_{34–50})¹⁷ which contacts the major groove of the bubble region. The flanking alanine residues were designed to increase α -helical content, and the *N*-terminal cysteine was included to allow future modifications. Closely related peptides have previously been shown to bind with high specificity to short model RNA sequences¹⁸ incorporating the Rev-binding domain of RRE. When solutions of Rev27 were injected under conditions of high stringency (10 °C, pH 7.4, 150 mM NaCl, 150 mM Na₂SO₄), selective formation of a 1:1 complex was observed for wt-RRE-II ($K_d = 215 \pm 10$ nM) and RBE3 ($K_d = 490 \pm 30$ nM), but not for RBE3-neg or Neo16-bd (Figure 4A,B). Under less stringent buffer conditions (10 °C, pH 7.4, 300 mM NaCl) the binding strength is significantly increased while the selectivity remains high. However, under these conditions only an upper limit can be derived for the dissociation constant ($K_d < 10$ nM at 5 °C) due to surface transport limitations.¹⁹ At higher concentration nonspecific binding is observed to all three sequences. The binding strength and selectivity²⁰ are somewhat higher at lower temperature (Figure 4C). This trend is consistent with previous observations by gel-shift experiments and can be explained by the higher α -helical content of the peptide at lower temperature. The CD spectrum of Rev27 at 5 °C has two minima at 222 and 210 nm characteristic of an α -helical structure. From the molar ellipticity at 222 nm an α -helical content of 64% at 5 °C was determined.²¹ Raising the temperature gradually unfolds the helix, and at 30 °C the α -helical content is reduced to 29%.

Binding of Aminoglycosides. Figure 5A shows the titration curve of neomycin B with wt-RRE-II, RBE3, and RBE3-neg. Binding of the aminoglycoside to all three RNA oligonucleotides is observed starting in the low nanomolar concentration range and is nonsaturable over the concentration range investigated. No significant changes to the binding isotherm were observed in the presence of 2 mM Mg²⁺, suggesting that the binding and the structure of the RNA hairpin are not influenced by divalent metals. The high degree of nonspecific binding is not surprising considering that aminoglycosides are highly charged polycations

(12) Peterson, R. D.; Bartel, D. P.; Szostak, J. W.; Horvath, S., J.; Feigon, J. *Biochemistry* **1994**, *33*, 5357.

(13) (a) Bartel, D. P.; Zapp, M. L.; Green, M. R.; Szostak, J. W. *Cell* **1991**, *67*, 529–536. (b) Cook, K. S.; Fisk, G. J.; Hauber, J.; Usman, N.; Daly, T. J.; Rusche, J. R. *Nucleic Acids Res.* **1991**, *19*, 1577–1582. (c) Iwai, S.; Pritchard, C.; Mann, D. A.; Karn, J.; Gait, M. J. *Nucleic Acids Res.* **1992**, *24*, 6465–6472.

(14) Battiste, J. L.; Mao, H.; Rao, N. S.; Tan, R.; Muhandiram, D. R.; Kay, L. E.; Frankel, A. D.; Williamson, J. R. *Science* **1996**, *273*, 1547–1551.

(15) (a) Wallis, M. G.; von Ahsen, U.; Schroeder, R.; Famulok, M. *Chem. Biol.* **1995**, *2*, 543. (b) Famulok, M.; Hüttenhofer, A. *Biochemistry* **1996**, *35*, 4265.

(16) (a) Mulligan, J. F.; Groebe, D. R.; Witherell, G. W.; Uhlenbeck, O. C. *Nucleic Acids Res.* **1987**, *15*, 8783. (b) Milligan, J. F.; Uhlenbeck, O. C. *Methods Enzymol.* **1989**, *180*, 51.

(17) (a) Malim, M. H.; Böhnlein, S.; Hauber, J.; Cullen, B. R. *Cell* **1989**, *58*, 205–214. (b) Malim, M. H.; Cullen, B. R. *Cell* **1991**, *65*, 241–248. (c) *Proc. Natl. Acad. Sci. U.S.A.* **1991**, *88*, 7734–7738.

(18) (a) Battiste, J. L.; Tan, R.; Frankel, A. D.; Williamson, J. R. *Biochemistry* **1994**, *33*, 2741. (b) Tan, R.; Chen, L.; Buettner, J. A.; Hudson, D.; Frankel, A. D. *Cell* **1993**, *73*, 1031. (c) Kjems, J.; Calnan, B. J.; Frankel, A. D.; Sharp, P. A. *EMBO J.* **1992**, *11*, 1119.

(19) Surface transport limitations have two important consequences: (1) at low concentration equilibrium cannot be reached during the length of the association phase which makes equilibrium measurements impossible and (2) kinetic measurements are not possible because the observed rates are not interaction controlled.

(20) Defined here as the ratio of specific to nonspecific binding when 1 equiv is bound specifically.

(21) Chen, Y.-H.; Yang, J. T.; Chau, K. H. *Biochemistry* **1974**, *13*, 3350.

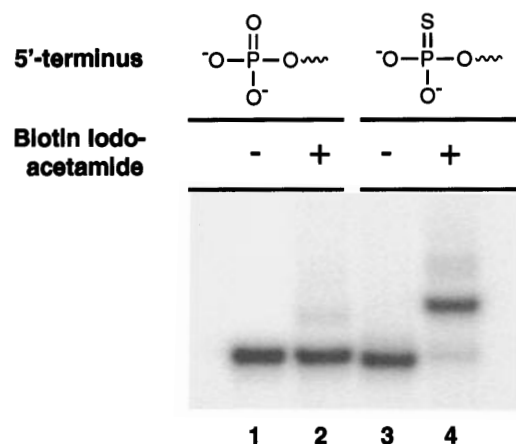
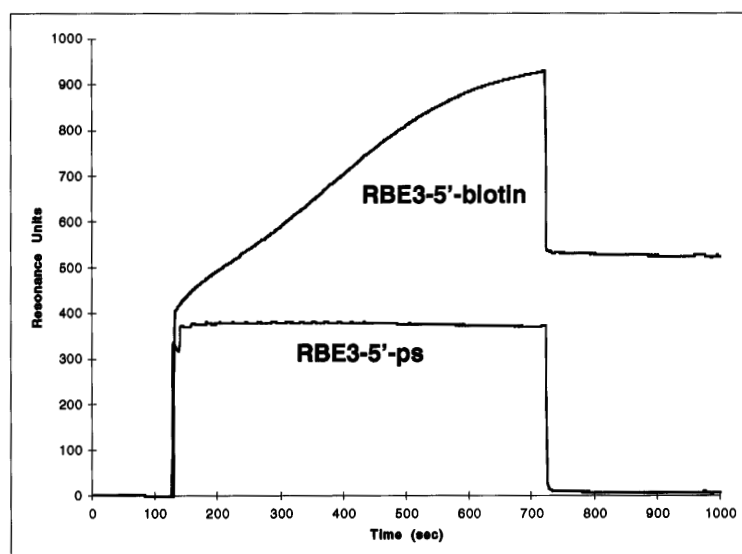
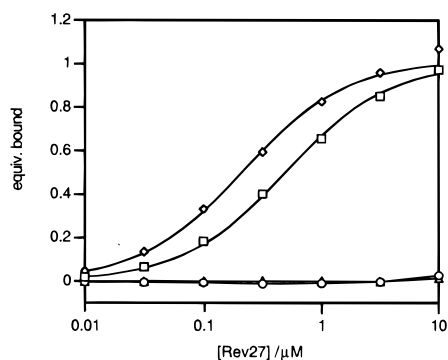
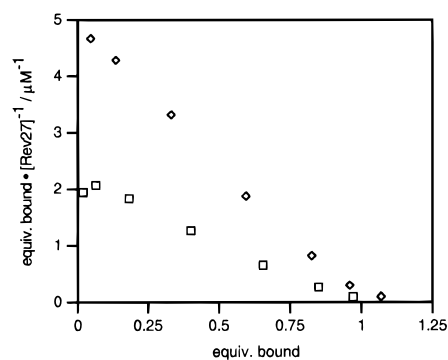
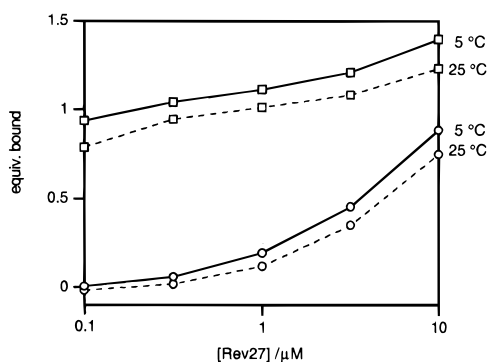
A Biotinylation Reaction**B Immobilization onto Streptavidin Chip**

Figure 3. Biotinylation and immobilization of RBE3 RNA. (A) Storage phosphor autoradiogram of a 20% denaturing polyacrylamide gel used to separate products of biotinylation reactions on ^{32}P -labeled RBE3-5'-phosphate and RBE3-5'-phosphorothioate (RBE3-5'-ps). Only the 5'-phosphorothioate containing RNA (lanes 3 and 4) is biotinylated. (B) Superposition of the injection traces for RBE3-5'-ps and RBE3-5'-biotin. Only the biotinylated RNA is successfully immobilized on the streptavidin-coated sensorchip surface.

A. Selectivity for Rev 27**B. Scatchard Plot****C. Temperature Dependence**

Rev27:
Suc-CAAAATRQARRNRRRRWRERQRAAAAR-NH₂

Figure 4. Binding selectivity for Rev27. (A) Titration curve under stringent conditions (pH 7.4, 10 mM HEPES, 3.4 mM EDTA, 5 mM DTT, 150 mM NaCl, 150 mM Na₂SO₄; $K_d(\text{wt-RRE-II}) = 200$ nM, $K_d(\text{RBE3}) = 430$ nM). (B) Scatchard plot of the data in (A). (C) Titration under lower stringency conditions at 5 °C (solid lines) and 25 °C (dashed lines) (pH 7.4, 10 mM HEPES, 3.4 mM EDTA, 5 mM DTT, 300 mM NaCl).

that tend to associate nonspecifically with the polyanionic phosphate backbone of RNA. A Scatchard plot of the data is shown in Figure 5B. The initial part of the plot reveals the presence of surface transport limitations at very low concentrations of neomycin B, which prevent reaching the equilibrium. This results in data points that lie systematically to the lower left of the true equilibrium curve. Data points corresponding to 0.5 equiv or more of neomycin B represent equilibrium values

and can be analyzed with respect to stoichiometry and affinity of aminoglycoside binding. Interestingly, there is no significant difference in the binding of neomycin B to RBE3 *vs* RBE3-neg. Both sequences bind one molecule of neomycin B with submicromolar affinity followed by weaker association with several additional equivalents of the antibiotic. This clearly shows that, while the G-rich bubble region is essential for Rev binding, it is not a determining factor for binding of neomycin

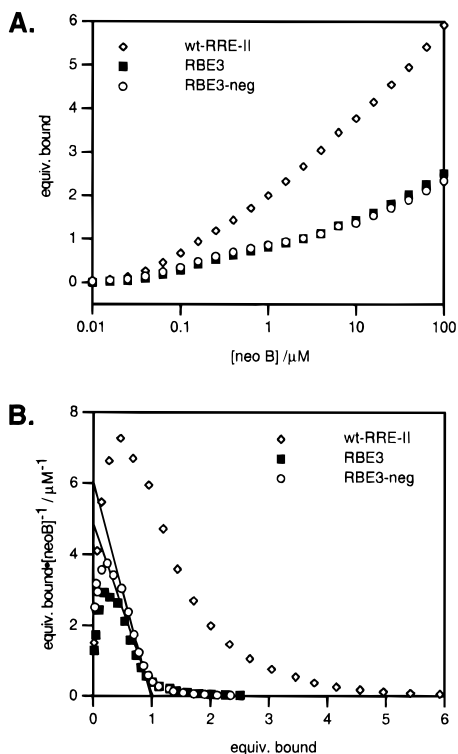


Figure 5. Neomycin B binding to RBE3, RBE3-neg, and wt-RRE-II. (A) Semilogarithmic plot. (B) Scatchard plot; (x -axis intercepts, 0.98 (RBE3-neg), 1.01 (RBE3); K_d values calculated from the slope, 160 nM (RBE3-neg), 210 nM (RBE3)). Conditions: pH 7.4, 10 mM HEPES, 150 mM NaCl, 3.4 mM EDTA, 25 °C.

B. Neomycin B either binds to a set of nucleotides within regular A-form RNA that is conserved between RBE3 and RBE3-neg or binds to the UUCG tetraloop that is not part of the wt-RRE sequence. In support of the latter possibility, selection experiments with RNA aptamers have established that aminoglycosides have a general affinity for stem loops,²² and these selection experiments have failed to identify any aminoglycoside-binding motif within regular double-stranded A-form RNA. However, recent footprinting experiments on comparable RNA hairpins have yielded no evidence of direct association to the UUCG tetraloop.

For wt-RRE-II, three molecules of neomycin B are bound with submicromolar affinity. Following the reasoning outlined above, it is possible that two of these molecules bind at the two hairpin loops present. The third equivalent might bind at the three-helix junction, overlapping with the binding site for the intact protein. This would be consistent with both the inhibitory effect of neomycin B on Rev–RRE binding and the reported footprinting data for binding of neomycin B in that region.

Paromomycin Binding. Another aminoglycoside that is closely related to neomycin B in structure but which has been reported to have virtually no inhibitory effect on the Rev–RRE binding is paromomycin (see Figure 1). The only difference between the two molecules lies in the replacement of neomycin's 6'-amino function with a hydroxyl group in paromomycin. As shown in Figure 6, equilibrium binding measurements did indeed show that paromomycin has approximately 15-fold lower affinity for wt-RRE-II, RBE3 and RBE3-neg compared to neomycin B. However, the relative affinity for the three sequences is unchanged, and the curves of the respective

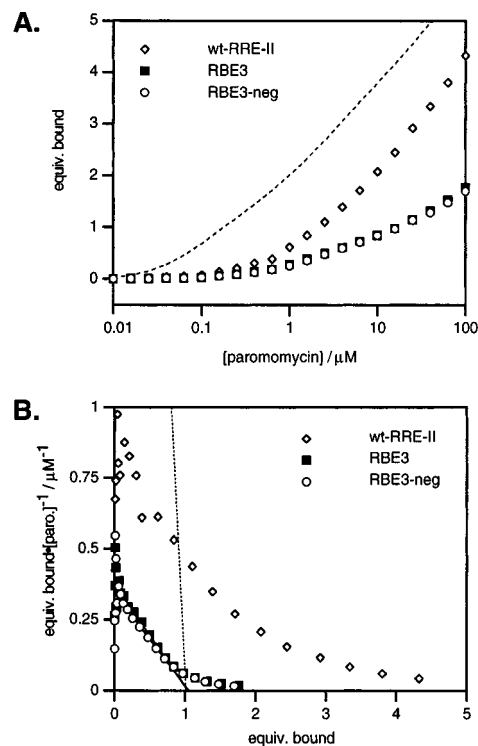


Figure 6. Paromomycin binding to RBE3, RBE3-neg, and wt-RRE-II. (A) Semilogarithmic plot. The dashed line indicates the binding of neomycin B to wt-RRE-II for comparison. (B) Scatchard plot. The dotted line represents the binding of neomycin B to RBE3; (x -axis intercepts, 1.05 (RBE3-neg), 1.04 (RBE3); K_d calculated from the slope, 3.1 mM (RBE3-neg), 2.8 mM (RBE3)). Conditions: pH 7.4, 10 mM HEPES, 150 mM NaCl, 3.4 mM EDTA, 25 °C.

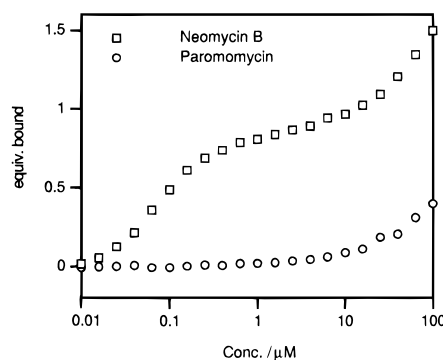


Figure 7. Kinetic stability of wt-RRE-II complexes with neomycin B *vs* paromomycin. Equilibrium was reached at the indicated concentrations of aminoglycoside, and then dissociation was effected by injecting aminoglycoside-free buffer (10 mM HEPES, pH 7.4, 150 mM NaCl, 3.4 mM EDTA). Data points were taken after 1 min of dissociation.

semilogarithmic plots are superimposable when shifted horizontally. This indicates that the specificity of binding is unchanged.

The difference in equilibrium binding affinity between neomycin B and paromomycin is too small to account for the extremely large reported inhibition differences observed in gel-shift assays (> 100-fold). However, careful examination of the dissociation phase revealed profoundly different dissociation kinetics for the two compounds. Data taken at different time points after switching from injecting aminoglycoside-containing buffer to aminoglycoside-free buffer represent time slices through the dissociation phase. Figure 7 shows the results obtained for wt-RRE-II after 1 min. The curve for neomycin B has the shape of an apparent 1:1 binding isotherm, contrasting with the shape of the equilibrium curve. This is due to the

(22) (a) Wang, Y.; Rando, R. R. *Chem Biol.* **1995**, *2*, 281. (b) Lato, S. M.; Boles, A. R.; Ellington, A. D. *Chem. Biol.* **1995**, *2*, 291. (c) Wang, Y.; Killian, J.; Hamasaki, K.; Rando, R. R. *Biochemistry* **1996**, *35*, 12338.

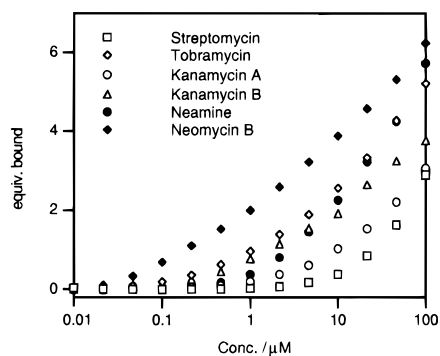


Figure 8. Comparison of equilibrium binding to wt-RRE-II for various aminoglycosides.

different dissociation rates for specific and nonspecific binding, with nonspecifically bound molecules dissociating much faster. Even more interesting is the difference between the two aminoglycosides: No apparent 1:1 binding isotherm is discernible for paromomycin, implying that the high-affinity binding sites for paromomycin within RRE are characterized by off-rates that are at least as fast as those of nonspecifically bound molecules. The same trend shown here for wt-RRE-II was also observed for RBE3 and RBE3-neg. Thus, it is apparent that while the equilibrium binding values do not reflect a large difference between these two closely related aminoglycosides, their dissociation kinetics are very different and may account for the large difference in inhibitory potency that has been observed by gel shift. Interestingly, these observations are also consistent with our previous finding in model systems that the 1,3-hydroxyamine substructure of the *gluco*-ring is an effective recognition element for phosphodiester.²³ Altering this substructure may therefore change binding.

Other Aminoglycosides. We have examined a number of other aminoglycosides belonging to the neomycin family, as well as streptomycin, an unrelated aminoglycoside antibiotic (Figure 1). Substantial differences exist with respect to their binding affinity for wt-RRE-II, spanning from neomycin B, which has the highest affinity, to streptomycin, which is weakest (Figure 8). All show nonsaturable binding in the micromolar concentration range. The same trend that was observed for wt-RRE-II was seen with RBE3 and RBE3-neg. The observed affinities for different aminoglycosides largely correlate with the total number of amines on the molecule and therefore with the overall charge.

Influence of Competing Ions. The binding of aminoglycosides to RNA is likely to involve substantial ionic contributions and therefore should be strongly influenced by competing buffer ions. In agreement with this notion, the inhibitory effects of aminoglycosides on ribosomal protein synthesis *in vitro* decrease with higher ionic strength of the medium.²⁴ Likewise, a strong salt dependence has been found for the inhibitory activity of neomycin B on hammerhead ribozyme activity. We studied the salt dependence of neomycin B binding to RBE3, RBE3-neg, and Neo16-bd (Figure 9) by varying the concentration of NaCl included in the injection buffer (10 mM HEPES, pH 7.4, 0.1 mM EDTA). At low concentrations of NaCl (100 or 50 mM) an increase in the amount of nonspecific binding was observed. However, at low ionic strength mass transport to the surface became an association rate limiting factor and at low concentrations of neomycin B equilibrium could not be

reached during the usual length of the association phase (10–20 min). At higher salt concentrations (200 and 250 mM) binding was sharply reduced for both RBE3 and RBE3-neg. The behavior of Neo16-bd under these conditions is especially interesting. This neomycin binding motif was obtained by *in vitro* selection under conditions of high ionic strength. At 250 mM NaCl Neo16-bd still shows strong binding to neomycin B. Under these conditions the selectivity for binding Neo16-bd *vs* RBE3 or RBE3-neg is approximately 100-fold. Interestingly, this advantage of Neo16-bd does not exist under less stringent salt conditions. Rather, it seems that specific binding to Neo16-bd is insensitive to ionic competition, whereas the binding to RBE3 and RBE3-neg is competed off by buffer salts. The nonspecific binding is sensitive to increasing ionic strength in both cases.

Discussion

Although it has long been known that aminoglycosides have a general affinity for RNA, much remains uncertain about their mechanism of action.²⁵ Their bactericidal effects are thought to be due to interference with the proper functioning of the prokaryotic ribosome. Several antibiotic binding sites have been identified by footprinting on the *E. coli* 16S ribosomal RNA.²⁶ Aminoglycosides of the neomycin family bind to the A-site of the ribosomal decoding region and induce translational misreading.²⁷ Very recently an NMR structure of the complex of paromomycin with an A-site analog RNA hairpin has been reported.²⁸ Paromomycin sits in a pocket created by a bulged residue and a noncanonical A:A base pair, stacking against the underside of another base pair. Specific contacts are formed to hydrogen bond acceptors in the RNA major groove and certain phosphates, including the apparent tridentate interaction of one amine and two hydroxyl groups with a particular phosphodiester oxygen. A few other naturally occurring aminoglycoside-binding sites have also been discovered. In addition to the HIV regulatory sequences RRE and TAR, these include the group I intron²⁹ and hammerhead ribozyme,³⁰ both of which interact most strongly with neomycin B. Other aminoglycoside-binding RNA sequences have been derived by *in vitro* selection, stimulated in part by the hypothesis that antibiotics may have played a role in the evolution of an RNA world as so-called low-molecular-weight effectors.³¹

A number of different methods have been employed for studying the interaction of aminoglycoside antibiotics with their RNA targets. These can be divided into two categories: (1) indirect observation through inhibition of protein binding or

(25) (a) Tanaka, N. *Mechanism of Action of Aminoglycoside Antibiotics. Handbook of Experimental Pharmacology*; Springer-Verlag: New York, 1982; Vol. 62, p 221. (b) Cundliffe, E. Recognition Sites for Antibiotics within rRNA. In *The Ribosome*; Hill, W. E., et al., Eds.; 1990; p 479. (c) Noller, H. F. *Annu. Rev. Biochem.* **1991**, *60*, 191.

(26) (a) Moazed, D.; Noller, H. F. *Nature* **1987**, *327*, 389. (b) Puhroit, P.; Stern, S. *Nature* **1994**, *370*, 659. (c) Recht, M. I.; Fourmy, D.; Blanchard, S. C.; Dahlquist, K. D.; Puglisi, J. D. *J. Mol. Biol.* **1996**, *262*, 421. (d) Miyaguchi, H.; Narita, H.; Sakamoto, K.; Yokoyama, S. *Nucleic Acids Res.* **1996**, *24*, 3700.

(27) Davies, J.; Davis, B. D. *J. Biol. Chem.* **1968**, *243*, 3312.

(28) Fourmy, D.; Recht, M. I.; Blanchard, S. C.; Puglisi, J. D. *Science* **1996**, *274*, 1367.

(29) (a) von Ahsen, U.; Davies, J.; Schroeder, R. *Nature* **1991**, *353*, 368. (b) von Ahsen, U.; Davies, J.; Schroeder, R. *J. Mol. Biol.* **1992**, *226*, 935. (c) von Ahsen, U.; Noller, H. F. *Science* **1993**, *260*, 1500.

(30) (a) Stage, T. K.; Hertel, K. J.; Uhlenbeck, O. C. *RNA* **1995**, *1*, 95. (b) Clouet-d'Orval, B.; Stage, T. K.; Uhlenbeck, O. C. *Biochemistry* **1995**, *34*, 11186.

(31) (a) Davies, J. *J. Mol. Microbiol.* **1990**, *4*, 1227. (b) Davies, J.; von Ahsen, U.; Schroeder, R. In *The RNA World*; Gesteland, R. F., Atkins, J. F., Eds.; Cold Spring Harbor Laboratory Press: New York, 1993, p 185. (c) Schroeder, R.; Streicher, B.; Wank, H. *Science* **1993**, *260*, 1443. (d) Hirao, I.; Ellington, A. D. *Curr. Biol.* **1995**, *5*, 1017.

(23) Hendrix, M.; Alper, P. B.; Priestley, E. S.; Wong, C.-H. *Angew. Chem., Int. Ed. Engl.* **1997**, *36*, 95.

(24) (a) Amils, R.; Ramirez, L.; Sanz, J. L.; Marín, I.; Pisabarro, G.; Ureña, D. *Can. J. Microbiol.* **1989**, *35*, 141. (b) Marín, I.; Abad, J. P.; Ureña, D.; Amils, R. *Biochemistry* **1995**, *34*, 16519.

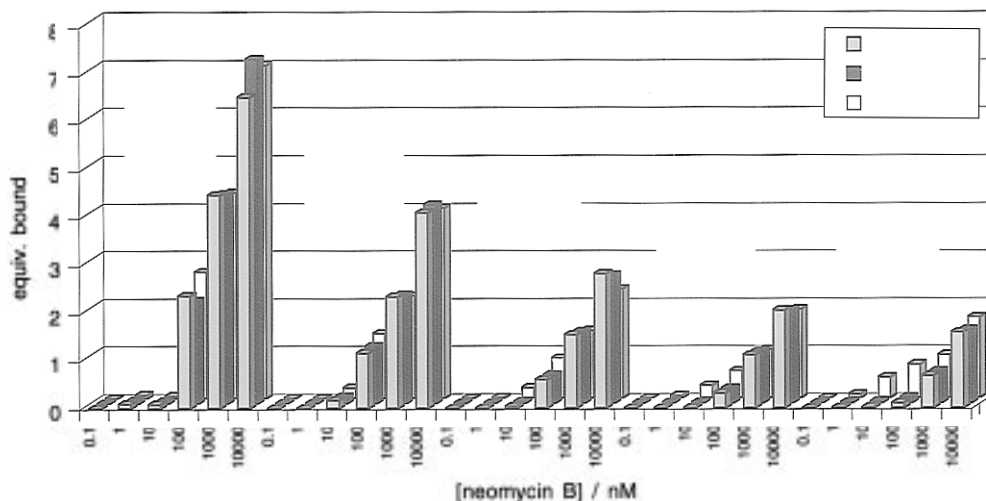


Figure 9. Influence of ionic strength on binding of neomycin B to RBE3, RBE3-neg, and Neo16-bd. Conditions: 10 mM HEPES (pH 7.4), 0.1 mM EDTA and NaCl as indicated.

catalytic activity and (2) direct binding assays. While indirect assays are usually reliable and sensitive, they cannot probe for specificity. A direct technique that has been frequently applied is chemical modification/protection using primer extension to detect the sites of interaction. This technique has the advantage of yielding some structural information. Its drawbacks lie in the limited choice of experimental conditions, use of radioactively labeled RNA, and number of experimental steps involved in each assay. Methods based on radioactively or fluorescently labeled aminoglycosides introduce a modification into the molecule that may affect its binding properties. With molecules as small as the aminoglycosides this is a serious concern. The same is true for experiments that require immobilization of the aminoglycoside on a column.

Other direct binding assays have been reported based on the separation of free RNA from aminoglycoside–RNA complexes using either polyacrylamide gel electrophoresis or ultrafiltration. Both methods rely on the kinetic stability of the aminoglycoside–RNA complex over the time period that it takes to separate them. Using our SPR system, we have investigated the time course of RNA–aminoglycoside dissociation and have found that a significant degree of dissociation can be observed in as little as 30 s.

Comparing the direct observation of aminoglycoside binding through SPR to the above-mentioned techniques, a number of advantages can be identified. The assay is operationally simple and can easily be automated to ensure good reproducibility. It yields direct information on the stoichiometry of ligand binding, and it is generally applicable to any kind of ligand without the need for labeling or modification. A wide variety of solution conditions can be employed. However, a number of limitations exist. Specific immobilization of the RNA *via* modification of the 5′-phosphorothioate requires an additional synthetic step in the preparation of the RNA. In principle, the immobilization matrix including the streptavidin–biotin complex may interfere with ligand binding, although no such difficulties were encountered in this study. Furthermore, kinetic limitations at low ligand concentrations, through either interaction kinetics or surface transport kinetics, may prevent the attainment of equilibrium in a reasonable time frame. Fortunately, the interaction kinetics of aminoglycosides are generally quite fast in the concentration range of interest (> 100 nM), and if equilibrium is not reached, it can be detected and taken into account. Analysis of the equilibrium response data through Scatchard plots seems particularly useful for both the simple detection of nonequilib-

rium data points and the determination of binding constants and stoichiometry.

Analysis of binding curves obtained with aminoglycosides reveals the presence of nonsaturable binding in the micromolar range for all RNA sequences studied. These results make intuitive sense given the polyionic character of these molecules. Similarly, a large number of nonspecific aminoglycoside binding sites has been found by equilibrium dialysis measurements on intact ribosomes.³² High-affinity binding with defined stoichiometry was found in the nanomolar range for all sequences. No significant difference exists in the binding of neomycin B to RBE3 and RBE3-neg. This contrasts sharply with the high selectivity of Rev-peptide binding to the same sequences, ruling out a specific recognition of the G-rich bubble region of RRE by neomycin. Taken together with the fact that up to three molecules of neomycin B are bound to the longer wt-RRE-II at submicromolar aminoglycoside concentrations, the results suggest that neomycin B may generally bind with this affinity to regular A-form duplex RNA or hairpin loops.

The relative lack of specificity for the interaction between neomycin B and wt-RRE-II, RBE3, or RBE3-neg is not surprising considering that neomycin B has not been produced in nature for the purpose of binding to RNA sequences in HIV. Any inhibitory effect is therefore likely to be accidental and not a specific, optimized recognition event. In this regard, the comparison of the RRE-related sequences and Neo16-bd is instructive. The latter RNA hairpin has evolved in the laboratory to bind neomycin B under conditions of high salt. In accordance with this selection pressure, Neo16-bd has an evolved binding site that is largely insensitive to competing ions. This is in contrast to the RRE-related sequences, for which binding decreases strongly with increasing ionic strength.

An interesting aspect of aminoglycoside binding to RNA which can be readily studied by our method is the substantial difference in dissociation kinetics between neomycin B and paromomycin. Whether these differences are functionally significant for the activity of aminoglycoside antibiotics remains to be seen and will be the subject of future studies.

Experimental Section

General Procedures. Surface plasmon resonance measurements were performed using a BIAcore 2000 system from Pharmacia Biosensor AB. Circular dichroism spectra were measured on an AVIV

(32) LeGoffic, F.; Capmau, M.-L.; Tanguy, F.; Baillarge, M. *Eur. J. Biochem.* **1979**, *102*, 73.

Model 62DS spectropolarimeter. UV spectra were taken on a Beckman DU650 spectrophotometer.

Synthesis of Biotinylated RNA. *In vitro* transcription reactions were performed according to the general procedure reported by Uhlenbeck and co-workers.¹⁶ The DNA templates (for wt-RRE-II, 5'-GCA CTA TAC CAG ACA ATA ATT GTC TGG CCT GTA CCG TCA GCG TCA TTG ACG CTG CGC CCA TAG TGC CTA TAG TGA GTC GTA TTA-3'; for RBE3, 5'-GGT GTA CCG TCA GCC GAA GCT GCG CCC ACC TAT AGT GAG TCG TAT TA; for RBE3-neg, GGT GTC CGC AGC CGA AGC TGC GGA CAC CTA TAG TGA GTC GTA TTA; for Neo16-bd, GGC GTC CTA AAC TTC TCG CCC AGG ACG CCT ATA GTG AGT CGT ATT A) were annealed to a 2-fold excess of 18-mer T7 promoter (TAA TAC GAC TCA CTA TAG) in H₂O by heating to 65 °C and slow cooling to below 37 °C. The 5'-phosphorothioate transcripts were generated by incubating the annealed templates (0.2 μM) in 50 mM Tris (pH 7.5), 15 mM MgCl₂, 2 mM spermidine, 5 mM DTT, 2 mM ATP, 2 mM CTP, 2 mM UTP, 0.2 mM GTP, and 4 mM guanosine-5'-monophosphorothioate (5'-GMPS) with 5 U/μL T7 RNA polymerase and 0.001 U/μL inorganic pyrophosphatase for 2 h at 37 °C in a total volume of 100 μL. Additional 1 μL aliquots of 20 mM GTP were added at 20 min intervals, and 500 U of T7 RNA polymerase was added after 1 h. Reactions were quenched by addition of EDTA, extracted with phenol, and precipitated with ethanol. Electrophoresis was carried out on 20% denaturing polyacrylamide gels. Full-length transcripts were excised from the gel and eluted into 200 mM NaCl, 10 mM Tris (pH 7.5), and 0.5 mM EDTA and desalted on a Nensorb column (DuPont/NEN). Typically, a 100 μL transcription reaction produced 150–500 pmol of RNA-5'-phosphorothioate. The purified RNA transcripts were resuspended in 18 μL of 100 mM NaH₂PO₄ (pH 8.0) containing 1 mM EDTA and were treated with 2 μL of 20 mM biotin-iodoacetamide in DMF (USB). After 2 h at room temperature, an additional 2 μL of the biotinylation reagent was added and incubation was continued for 1 h. The RNA was ethanol precipitated in the presence of glycogen, gel purified, and desalted as described above. The RNA oligonucleotides for the gel in Figure 2 were body labeled by incorporation of [α -³²P]ATP (0.4 μCi/μL) in the transcription reactions containing either 5'-GMP or 5'-GMPS.

Immobilization of Biotinylated RNAs on the Sensorchip. Streptavidin-functionalized BIAcore sensorchips were either obtained directly from Pharmacia Biosensor AB (sensorchip SA5) or prepared from carboxymethylated sensorchips (CM5) by EDC activation followed by injection of streptavidin (Pierce, immunopure grade) in acetate buffer (10 mM, pH 5) over all four flow cells according to the manufacturer's recommendations. Prior to immobilization, frozen solutions of biotinylated RNA (1–10 pmol) in 80 μL of buffer (10 mM HEPES, 0.1 mM EDTA, 100 mM NaCl, pH 6.8) were renatured by heating to 80 °C for 2 min followed by slow cooling to room temperature. Typically, individual flow cells were functionalized by injecting 60 μL of RNA buffer using the QUICKINJECT command at a flow rate of 2 μL/min, followed by injection of running buffer. Three flow cells were used to immobilize RNA while the fourth remained unmodified to serve as a blank control for matrix affects. Levels of RNA capture and ligand binding were calculated by subtracting response units of the blank flow cell from response units in the RNA functionalized flow cells.

General Procedures for SPR Binding Studies. Samples were prepared by serial dilutions from stock solutions in RNase free microfuge tubes (Ambion) and were centrifuged at 14 000 rpm for degassing. Buffers were filtered through sterile 0.2 μm nylon membranes (Nalgene) under vacuum, except for BIA- certified HBS buffer (Pharmacia Biosensor AB) which was used as obtained. All procedures for binding studies were automated as methods using repetitive cycles of sample injection and regeneration. Typically, buffer was injected in the first two cycles to establish a stable baseline value. Samples were injected at a flowrate of 5–10 μL/min using either the KINJECT or the COINJECT command. All aminoglycoside and Rev27

samples were injected from autoclaved 7 mm plastic vials that were capped with pierceable plastic crimp caps. To minimize carryover, samples were injected in order of increasing concentration. The running buffer was identical to the injection buffer, except for the salt dependence study where a single running buffer was used for all injections. Expected values for the equilibrium response of 1 equiv of analyte were calculated from the relative molecular weight of the analyte and the immobilized RNA ligand in each flow cell. These values were adjusted by multiplying with a factor of 0.8 or 0.57 for Rev27 or aminoglycosides, respectively. These factors arise from the different molar refractive indices of RNA and the analyte which translate into a different SPR response per unit concentration change. The factors were determined from the Scatchard plot *x*-axis intercepts of the 1:1 binding isotherms for Rev27 and neomycin B. The values of the factors reflect the order of molar refractive indices of RNA > peptide > aminoglycoside and are in line with expectations.³³

Binding Studies with Rev 27. Rev27 was obtained from QCB Inc. (Hopkinton, MA). Analytical data (HPLC, capillary electrophoresis, MS) were in agreement with the structure and indicated a purity of >95%. Aliquots of a stock solution of Rev27 (100 μM) in injection buffer (10 mM HEPES, pH 7.4, 150 mM NaCl, 3.4 mM EDTA, 5 mM DTT) were stored frozen (–30 °C) until used, and samples were made up freshly by serial dilution in injection buffer. Data points were taken after an association phase of 20 min. A 3 min regeneration pulse of 300 mM Na₂SO₄ in injection buffer was used between injections. Binding constants for RBE3 and wt-RRE-II were from nonlinear curve fitting to the equation $\text{Resp} = \text{Resp}_{\text{max}}[\text{Rev27}]/([\text{Rev27}] + K_d)$ wherein Resp is the observed response and Resp_{max} is the response of 1 equiv of Rev27 bound.

CD Spectra of Rev27. Samples were made up freshly from stock solutions of Rev27 (0.1 mM) in CD buffer (10 mM potassium phosphate, pH 7.5, 100 mM KF) using a 1 cm path length quartz cuvette. The signal was averaged over 30 s, and 5 scans of the full spectrum were averaged. The concentration of Rev27 was determined from its UV spectrum using the absorption at 279.8 nm due to the single tryptophan residue. The helical content was calculated from the mean residue ellipticity at 222 nm relative to the expected value at full α -helicity (35 740 (deg·cm²)/dmol for a 27-mer).

Binding Studies with Aminoglycosides. Neomycin B sulfate (Fluka) was converted to the free base by passing it through Amberlite IRA 400 (OH[–] form) and purified by ion exchange chromatography on Dowex 1-X2 100 to remove neomycin C;³⁴ the purity of neomycin B was verified by NMR in D₂O. Paromomycin sulfate was obtained from Sigma and used as received. Samples were prepared by dilution from 10 mM stock solutions in injection buffer (10 mM HEPES, pH 7.4, 150 mM NaCl, 3.4 mM EDTA). Data points were taken after an association phase of 30 min. A 2 min regeneration pulse of 150 mM Na₂SO₄ in injection buffer was used between injections. Binding constants for RBE3 and RBE3-neg were obtained by fitting the linear part of the Scatchard plot to a straight line (slope = $-1/K_d$).

Acknowledgment. This project was supported by Sandoz Pharma, Ltd. E.S.P. gratefully acknowledges the National Institutes of Health for a postdoctoral fellowship.

Supporting Information Available: CD spectrum of Rev27, temperature dependence of the α -helical content of Rev27, and sensogram overlay for neomycin B binding to RBE3 (2 pages). See any current masthead page for ordering and Internet access instructions.

JA9642900

(33) *BIAtechnology Handbook*; Pharmacia Biosensor AB: Uppsala, 1994; Chapter 4.

(34) Umezawa, H.; Kondo, S. *Methods Enzymol.* **1975**, *43*, 263.